DETAILED DISC ASSEMBLY TEMPERATURE PREDICTION: COMPARISON BETWEEN CFD AND SIMPLIFIED ENGINEERING METHODS

ISABE-2005-1130

Glen Snedden, Thomas Roos and Kavendra Naidoo

CSIR, Defencetek, P O Box 395
Pretoria, 0001, South Africa
gsnedden@csir.co.za

Abstract

Previous simulations of a turbojet disc cavity (Snedden 2003) with full Navier-Stokes CFD and simplified geometry and boundary conditions have been improved to reduce the level of approximation. A new grid was built using a multi-block approach. The case was computed with a commercial Navier-Stokes solver, **STAR-CD** (CD-Adapco Group), on the latest parallel computing system available at the CSIR. These results will be compared to those computed with an in-house developed 1-D flow solver coupled with a 3D conduction code, and thermal paint validation data. The aim of the paper is to review the approach to disc cavity analysis followed by the CSIR.

Nomenclature

CAD	Computer Aided Drawing
CFD	Computational Fluid Dynamics
DCOOL	3D Finite Difference Conduction Code
FEM	Finite Element Method
h	Heat Transfer Coefficient
ICP	1D Network Flow Solver
N-S	Navier-Stokes
TACT1	Internal impingement, coolant flow and heat transfer and conduction code (Gaugler, 1978)
T_{aw}	Adiabatic Wall Temperature
y+	Near wall Reynolds number

Introduction

In order to calculate life degradation of gas turbine disc assemblies, it is necessary to model the transient thermal and mechanical stresses experienced by the components through an idealised or experimentally measured mission cycle. These stresses are calculated using a transient FEM analysis taking into account all appropriate constraints to expansion, as well as both elastic and plastic deformation. An important component of this analysis is the transient thermal loading on the disc assembly. The predominant thermal loading is convective: the heating which takes place at the disc rim by conduction through the fir-trees from the blades in the hot gas flow path, and the cooling which takes place on the disc upstream and downstream faces as a result of coolant air bled from the compressor swirling in the disc cavities. Less dominant, but still significant, is the effect of conduction to adjacent components attached by bolting or pressfit to the discs.

CFD is ideally suited to investigate conjugate heat transfer in a complex convective heat transfer problem such as a disc assembly, but the combination of multiple discs, each with their own integer non-axisymmetric geometric features such as bolt-heads, blade shanks and disc flow metering holes, rapidly escalate the scale of the CFD model to impractical levels without significant simplifications. A transient analysis, particularly through a typical mission profile, becomes impossible.

For this reason, simplified tools are more appropriate for the generation of the thermal boundary conditions for the FEM analysis mentioned earlier. Transient conduction is often calculated on an idealised 2D slice as a boundary condition for a transient conduction analysis. The convective analysis is performed for the design or takeoff condition, and possibly again for the idle condition, and interpolation between the two is used for other operating points.

Navier-Stokes CFD (with conjugate heat transfer) has been used at CSIR to explore flow field detail and assess the modelling requirements of specific coolant flow phenomena (Snedden and Lambert (2003)). Since simplified methods, as described above, are orders of magnitude faster to run and offer 2D/Quasi-3D solutions for engine transients, such a set of simplified tools has been in development at CSIR for several years. These in-house codes, **ICP** and **DCOOL**, comprise a network code for 1D flow solutions and a conduction code for the solution of metal temperature respectively.

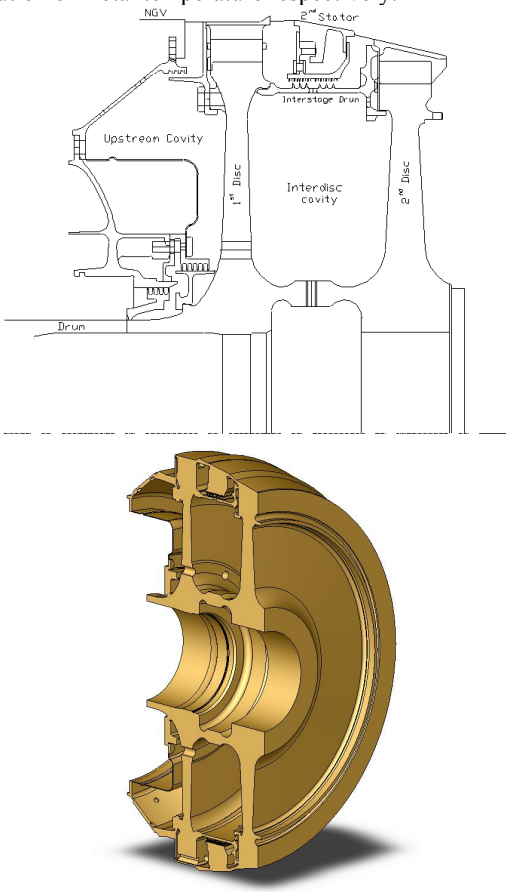

Figure 1: CAD assemblies

This paper aims to compare the relative merits of these two techniques against a single, complex validation case, that of Snedden (2003) (see Figure 1). In addition results of two separate Navier-Stokes solutions will be presented, the simplified solution of Snedden (2003), and a solution of a more detailed model computed with the parallel computer system at the CSIR. Both N-S solutions were computed with the commercial finite volume CFD package **STAR-CD**. These N-S CFD solutions will be compared to the results from the simplified coupled analysis with the in-house codes, **ICP** (network flow solution) and **DCOOL** (disc conduction).

Simplified Coupled Analysis

Tools Description: **DCOOL**

Conduction modelling philosophy

DCOOL is a structured mesh finite-difference, three-dimensional, conduction solver. The philosophy behind the code is the solution, at each iteration, of the temperature distribution of each of the disc assembly component meshes in turn. Temperatures required for conduction across the interface between adjacent contiguous components are updated each iteration.

The components modeled are all quasi-axisymmetric about the engine centerline (discs, shafts, labyrinth seals, curvic couplings etc), but are modeled as angular sectors to reduce mesh size and unnecessary repeating detail in the tangential direction. The sector is chosen so as to be representative of all the dominant geometric features in the tangential direction (blade shanks and disc holes).

Each component consists of three nodes across the thickness and a variable number of nodes in the other two directions, being tangential and radial in the case of discs and tangential and axial in the case of drum-shaped elements. In this respect it is similar to **TACT1** of Gaugler (1978) for impingement-cooled blades. Components in conductive contact must have the same number of nodes in the tangential direction. Any number of components can be modelled together.

The blades in the firtrees are regarded as part of the disc, with the blade platform surface forming the convective boundary in the hot gas flow path. The region between adjacent blade shanks is modelled in the same manner as any other hole in the disc: the individual nodes in hole regions are "blanked out", and are not "visible" to their neighbours as a conduction node. If a node is designated as falling in a hole, the interface between it and a solid region is regarded as a convective heat transfer surface, and the T_{aw} and h from the nearest **ICP** node to it is applied to that surface. The number and positions of each hole for each component are read in from a dedicated file. Contact resistances are read in from a separate dedicated file for the blade/disc firtree interface.

Boundary conditions

Boundary conditions available at the hub and bore of these components are

1) fixed temperature
2) adiabatic
3) fixed heat flux
4) convective heat transfer to coolant using T_{aw} and h calculated in **ICP** (the flow coolant network)
5) convective heat transfer from hot gas flow path using T_{aw} and h specified from the main gas flow path
6) conduction to another component

The boundary conditions at the tangential edges of the mesh sector are always cyclic, to ensure a periodic temperature distribution. A file read by the preprocessor determines which areas on the faces (as opposed to the hub or bore) receive convective heat transfer, T_{aw} and h from **ICP** and which from the main gas flow path. The values of T_{aw} and h from both **ICP** and the main gas flow path are interpolated onto the convective surfaces.

Solver

The solver makes use of an alternating-direction-implicit approach, using the tri-diagonal implicit algorithm. This is done since the solution matrix is so sparse.

Input files for the assembly are created and read by a preprocessor, which creates calculation coefficients for the solution matrices. This is done once. The solver **DCOOL** reads in these values as well as the latest output file from the coolant solver **ICP** and calculates an updated metal temperature distribution. Use is made of a temperature-dependant thermal conductivity, and for transient simulations, temperature-dependant specific heat capacity. Both these values are read in from a user-specified file for the particular material.

At interfaces between nodes use is made of the harmonic mean of the two node thermal conductivities rather than the arithmetic mean. This prevents falsely high conductive heat transfer between two nodes of greatly dissimilar conductivities, by biasing the interface conductivity toward the lower conductivity instead of taking a spatial interpolated value.

Tools Description: **ICP**

Convection modelling philosophy

The convection solver is called ICP and was originally the result of a Masters thesis (Lippert, 1994), based on the work of Meitner (1989). Originally written for the modelling of internally cooled blades with serpentine passages, turbulator strips and pin fins, it is a compressible one-dimensional solver that takes a form similar to that of a pipe flow network, except that it is restricted to branches splitting from the main branch which may reattach further down. It can handle rotation with the corresponding hydrostatic pressure gradient. It has been extensively upgraded at CSIR to be able to model disc cavity flows, and calculates core rotation factors in cavities.

Geometry

As in **DCOOL**, a sector of the engine volume of revolution is chosen. Two classes of node geometries are modelled: annuli and passages.

An annulus in this usage is an axisymmetric flow field where the flow proceeds unbounded in the tangential direction but radially bounded by walls at two different radii (as in a labyrinth seal) or else axially bounded by walls at two different axial positions (as between two discs) or finally some combination of these two. Geometry is specified by giving a node boundary point on the two bounding surfaces (as in annular gaps or

disc cavities) from which the line connecting the points is bisected to obtain the node centre coordinates, and the flow cross-sectional area is calculated by sweeping the line at the node radius across the sector angle.

A passage on the other hand is a flow completely bounded, such as pipe flow. The number of flow passages (such as between blade shanks) is specified at a given radius. The hydraulic diameter is given at different node positions, and the cross-sectional area is calculated based on that and the number of passages at that node.

Boundary conditions

Published heat transfer correlations are applied to different surfaces depending on the condition (rotor-rotor, rotor-stator, labyrinth seal, etc). The correlations of Owen for rotor-rotor (Northrop and Owen, 1988) and rotor-stator (Owen and Haynes, 1976; and Owen et al, 1974) and used.

Test Case Geometry

Fundamental challenges in modelling disc cavities are always the engineering choices needed to simplify the model to the point where it will yield a solution with acceptable, appropriate accuracy and is at the same time representative of the true geometry. The test case assembly geometry consists of two discs and an interconnecting drum rather than a spacer; however the complexity is in finding the lowest common denominator between the number of blades, coolant injection holes and other discrete features, so that the geometry is amenable to a periodic solution. Table 1 (the actual tangential feature count is indicated in brackets in the first column) illustrates this complexity while Figure 1 shows both the original axisymmetric model from Snedden (2003) and the updated 3D solid model created to explore the latest automatic meshing techniques available to the CFD user today.

Simplified Coupled analysis

The **DCOOL** model of the solid components closely resembles that of the simplified N-S model, comprising a 30° sector with the same number of blades, holes and the like as in the simplified N-S model. Included the conduction analysis was the interstage drum, visible in Figure 1.

The same wall boundary conditions of fixed temperature and adiabatic regions as in the detailed N-S were employed for comparison although more accurate platform temperature distributions can be modelled.

The **ICP** model comprised three flow branches (see figure 13): the main branch which approaches the 1st disc from the supply (with a simple pipe flow turbulent heat transfer boundary condition on the outer wall), is drawn down the front of the 1st disc (adiabatic stator and Owen's rotor model (Owen and Haynes, 1976; and Owen et al, 1974)), passes through the hole near the bore of the 1st stage disc (turbulent pipe flow again), enters the rotor rotor cavity (using Owen's rotor-rotor model (Northrop and Owen, 1988)) and passes out of the hole in the interstage drum. The second branch splits off from the main branch just before the interstage drum hole, passes through the holes in the 2nd stage disc coverplate, proceeds radially between the coverplate and the 2nd disc (using Owen's rotor-rotor model (Northrop and Owen, 1988)) before passing between the 2nd stage disc shanks (turbulent pipe). The third branch leaves the main branch - just upstream of being drawn radially inward upstream of the first disc - and instead proceeds radially outward (adiabatic stator and Owen's rotor model (Owen and Haynes, 1976; and Owen et al, 1974)), then passing between the 1st stage coverplate and disc (using Owen's rotor-rotor model (Northrop and Owen, 1988)) before passing between the 1st stage disc shanks (turbulent pipe).

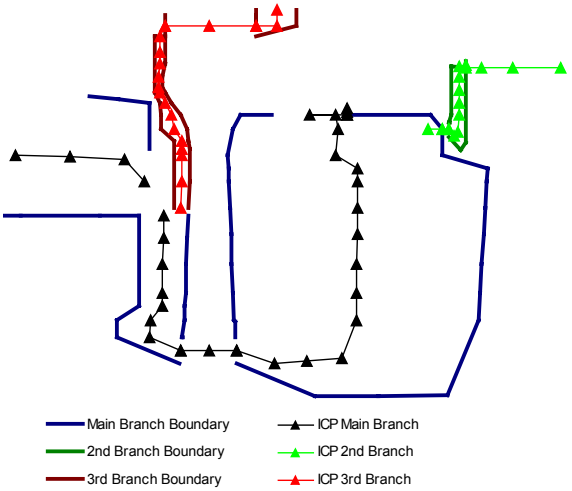

Figure 13: Representation of the **ICP** network

Navier-Stokes Analyses

A commercial finite volume CFD code, **STAR-CD** (CD-Adapco Group), was used for the computation of the flow field and temperature distribution in the disc assembly.

Three dimensional flow field variables are computed with the numerical solution of the Reynolds Averaged Navier-Stokes equations, energy equation, turbulence equations and the ideal gas law. The temperature field in the solid disc assembly was computed simultaneously with a special form of the energy equation used in the flow analysis. The convective terms in the governing energy equation for fluids are reduced to zero for the temperature solution in the metal. Heat flux continuity is enforced at the solid fluid interface to enable conjugate heat transfer between the fluid and solid regions in the domain of interest.

The effect of the disc assembly rotation is approximated with the aid of rotating reference frames, that is, addition of rotational terms in the cell volumes within an appropriate region of the solution domain. The bounds of this region are approximate and velocities across the interface are averaged at each iteration of the computation. Numerical solution is first-order accurate and computed with the SIMPLE algorithm.

Table 1 summarises the simplifications in the original CFD model of Snedden (2003) and the latest work. Table 1 also includes some of the resultant critical parameters such as y+, relative grid size and modelling philosophies.

Simplified Navier-Stokes Analysis (30° axisymmetric sector)

Figures 2 to 4 give an idea of the mesh, boundary conditions and flow solution for the simplified case. A

more detailed analysis of these results can be found in Snedden (2003).

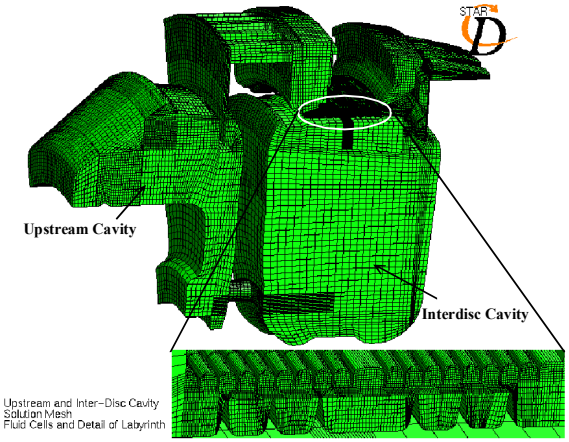

Figure 2: Simplified CFD fluid cell geometry

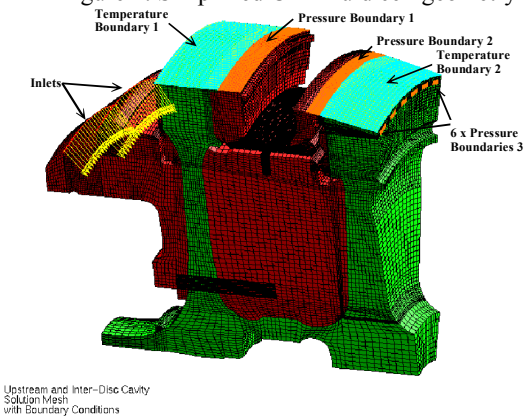

Figure 3: Overall geometry boundary conditions

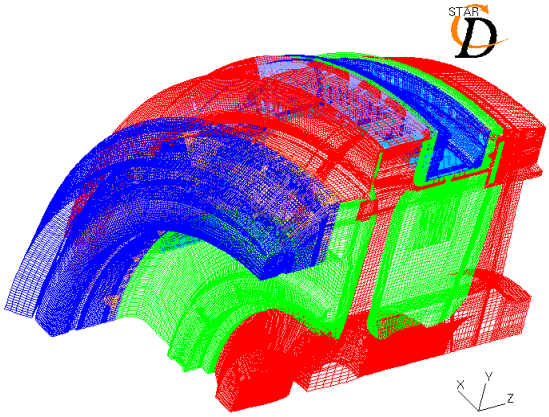

Figure 5: Complete CFD grid

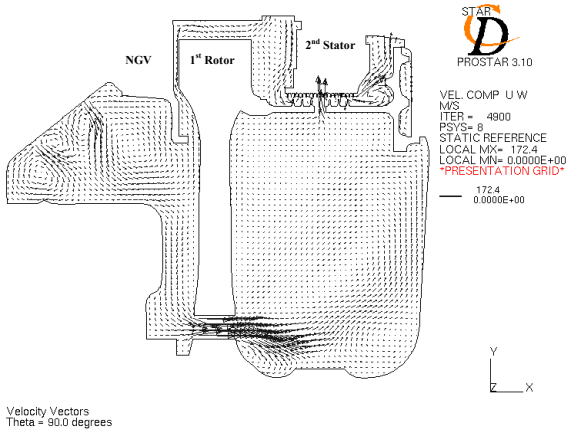

Figure 4: Overall flow pattern

Detailed Navier-Stokes Analysis (90° axisymmetric sector)

Automatic mesh generation with **STAR-CD** requires a "water-tight" surface that may be generated with Solid Works. The fine detail in the labyrinth seal and other discrete features requires careful manipulation of the initial surface to provide a high quality, accurate control surface surrounding the domain of interest. Automatic mesh generation techniques for a typical disc cavity assembly are currently being investigated.

For this study, a structured computational grid for the fluid and solid regions was generated with a multi-block approach (see Figures 5 to 8).

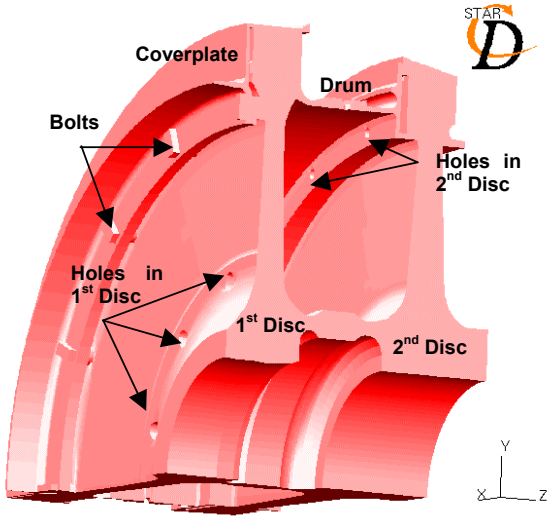

Figure 6: Plot of solid surfaces indicating tangential features

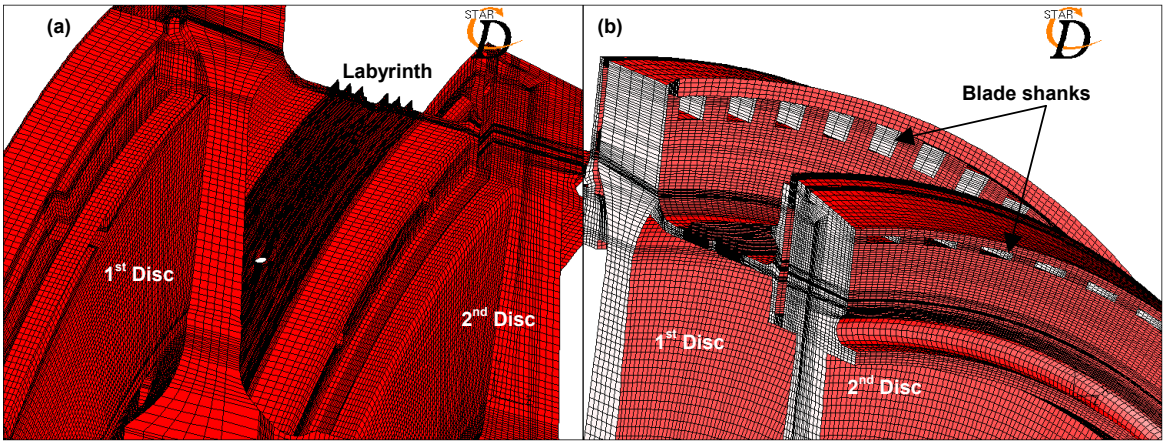

Figure 7: Magnified views of the grid highlighting geometrical features

Table 1: Comparison of Modelling Simplifications for both Navier-Stokes Solutions

Item Description	Simplified N-S Analysis	Detailed N-S Analysis
Geometry		
Sector	30°	90°
Holes in 1st Disc (12)	12	12
Holes into the labyrinth seal (15)	12*	16*
1st stage blades (83)	84	84
2nd stage blades (66)	72	68
Impingement hole onto 2nd disc (20)	24*	20
Lower Supply hole (21)	Modelled as slot	20*
Upper Supply hole (14)	Modelled as slot	12*
Bolts (16)	None	16, modelled with square heads
Inter-stage drum	Metal conduction not modelled	Modelled
	Numbers indicated are representative for 360° * Hydraulic diameters were adjusted appropriately, to accommodate mismatch with actual geometry	
Grid		
Solid Cells	220 000	2 600 000
Fluid Cells	58 000	1 200 000
y+	250 to 550	15 to 250 Shank holes and disc holes (500)
Flow Model		
Turbulence	k- ε, Turbulence Intensity = 5%, Length Scale = 0.01	
Viscosity	Sutherland's Law	
Conjugate heat transfer	Yes	
Boundary Conditions		
Supply	Fixed Inlet mass-flow rate through the supply holes with a percentage of the coolant flow rate and an even distribution of it through either supply hole. Holes modelled as slots.	Pressure boundary on plenum upstream of discrete supply holes.
Main Gas Flow Path Interfaces	Static pressure boundaries	Static pressure boundaries
Blade platforms	Fixed temperature	Fixed temperature, 1st disc platform temperature reduced by 40° based on previous results and after further 3D analysis of the main gas flow path
Remaining walls	Adiabatic	Adiabatic
Material Properties		
Metal conductivity	Stainless 316	MAR-M 509
Contact resistances	Blade material and disc material in the fir tree region were assumed to be homogeneous and uninterrupted, that is, thermal contact resistance was not modelled	
Solver Accuracy	First-order accurate	First-order accurate

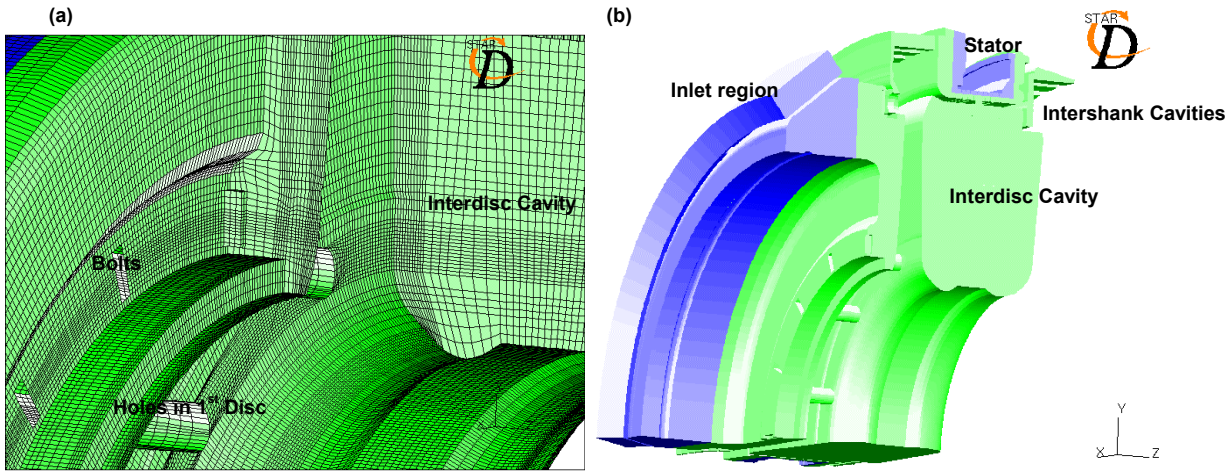

Figure 8: (a) Fluid grid (b) Surface plot of fluid grid indicating tangential features

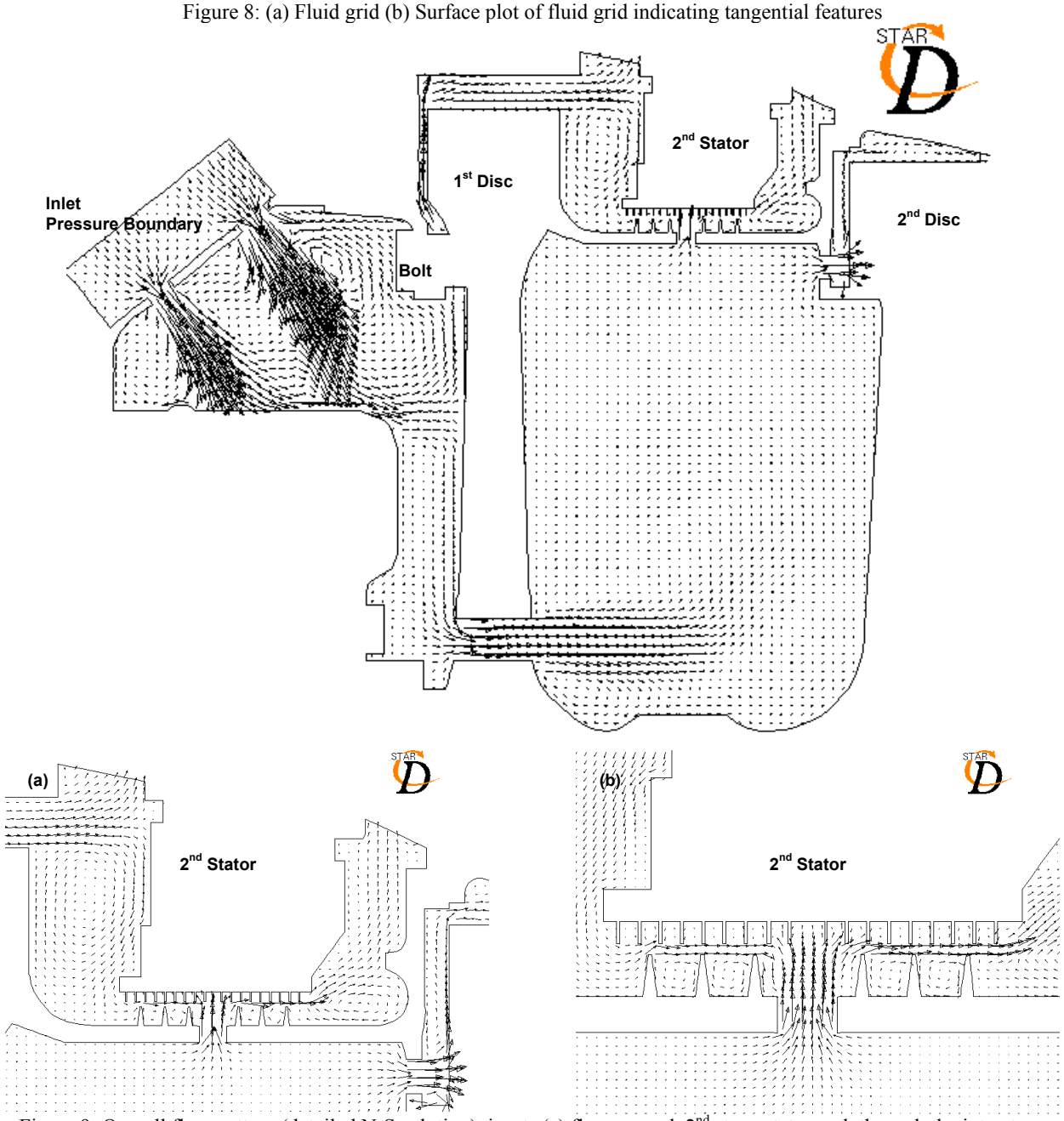

Figure 9: Overall flow pattern (detailed N-S solution), insets (a) flow around 2nd stage stator and through the interstage drum, (b) close in view of the labyrinth seal flow

Plenum inlet conditions are fixed at stagnation pressure and total temperature. Overall pressure drop across the assembly drives the flow through the supply holes. The flow reaches approximately Mach 0.9 (Figure 11) in the supply holes. Upper and lower supply hole diameters were increased by 16.7% and 5% respectively to maintain the total supply flow area of the actual geometry. It is possible that the holes are choked in the actual geometry.

The static temperature (Figure 10a) drops across the holes and in the supply jets due to the local acceleration of the flow, as one would expect. However, this is accompanied with an unexpected total temperature (Figure 10b) drop across the supply holes. This has the effect of further reducing the coolant temperature in the flow upstream of the first disc. This introduces artificial cooling at the base of the first and second discs. Independent tests performed on the inlet area alone reveal that the total temperature drop across the inlet holes is due to the coarse grid resolution in the supply holes and to a smaller extent to the use of a first-order accurate computation scheme.

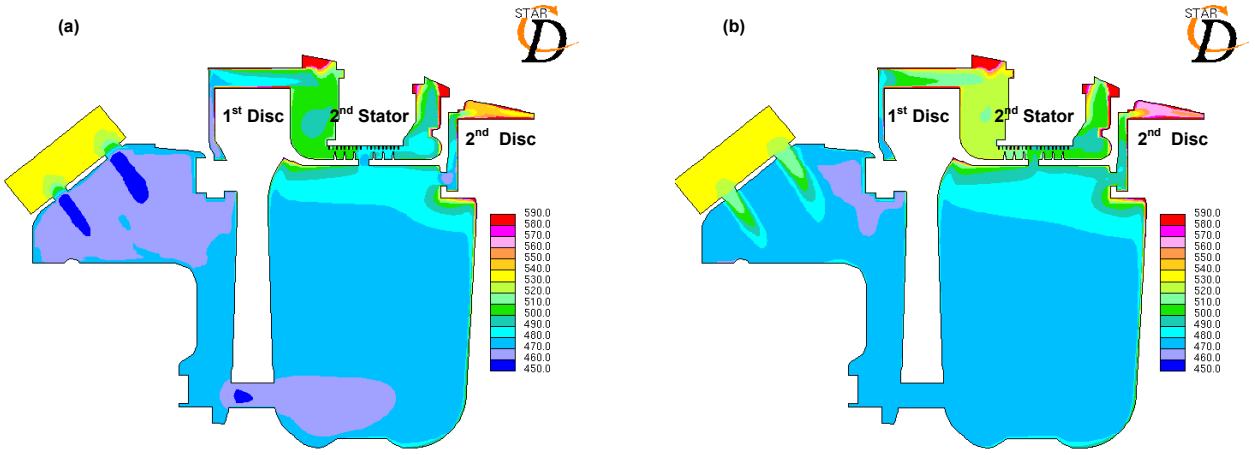

Figure 10: Detailed N-S solution (a) Static temperature, (b) Total temperature

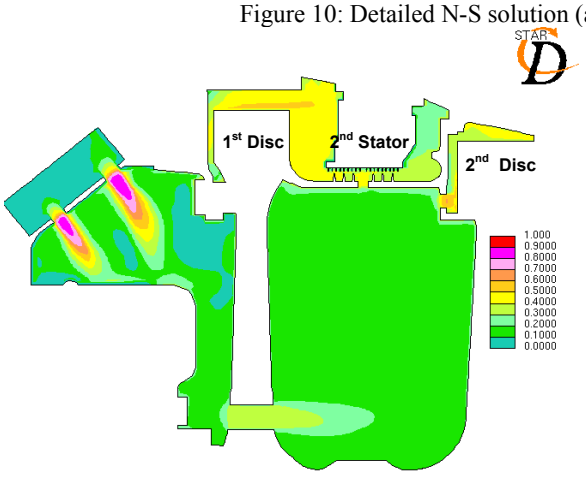

Figure 11: Detailed N-S solution, Mach No. distribution

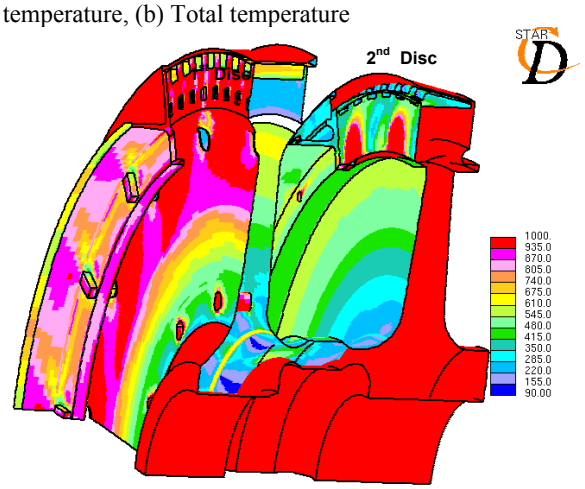

Figure 12: Detailed N-S solution, wall heat transfer distribution

The lower supply jet impinges on the lower wall and sets up a recirculation zone in the bottom corner of the entrance chamber. The flow also moves along the wall toward the upstream face of the first disc. The upper jet penetrates the flow in the entrance cavity and proceeds towards the face of the first disc. There is evidence of some grid dependence on the modelling of the upper jet. The jet penetration into the entrance cavity is slightly less due to the additional diffusion introduced by the sparse grid here. Supply flow is accelerated radially along the upstream face of the first disc into the inter-shank passage and towards the hole in the first disc.

In the entrance cavity/inlet flow region there are observable differences between the results of the latest N-S computation and those presented by Snedden (2003). In the previous simulation the inlet flow was modelled as a slot, with the total coolant mass flow rate fixed at the inlet boundary condition. In this case, total mass flow rate, was averaged over an annular inlet with a relatively larger cross sectional area. This will result in a smaller velocity at the supply inlet and hence a weaker supply jet in this plane. In the latest simulation, mass flow is driven by the pressure difference across the assembly over a much smaller supply inlet area, and should ideally

remove the need to make assumptions regarding the coolant massflow rate into the disc cavity such as those made by Snedden (2003).

Coolant flow from the hole in the 1st disc moves axially toward the 2nd disc and radially toward the hole in the 2nd disc as well as the hole in the labyrinth seal. Flow through the holes in the interstage drum impinge on the 2nd disc creating a local cooling effect. On the downstream face of the 1st disc, air is being pumped radially toward the inter-stage drum.

Flow from the inter-shank cavity on the 1st disc penetrates the flow between the 1st disc and stator. Flow impinging on the stator moves towards the main gas flow path and toward the labyrinth seal. In this region of the flow there is an observable difference on comparison to results presented by Snedden (2003). Low grid resolution in the inter-shank cavity on the 1st disc resulted in a larger static pressure drop across the passage and hence greater entrainment of hot gas from the main gas flow path. In the latest simulation there is less hot gas entrainment.

In the latest simulation a recirculation zone is setup between the 1st disc and stator. The remaining flow moves toward the labyrinth seal and toward the main gas flow path between the stator and 2nd disc blade platform.

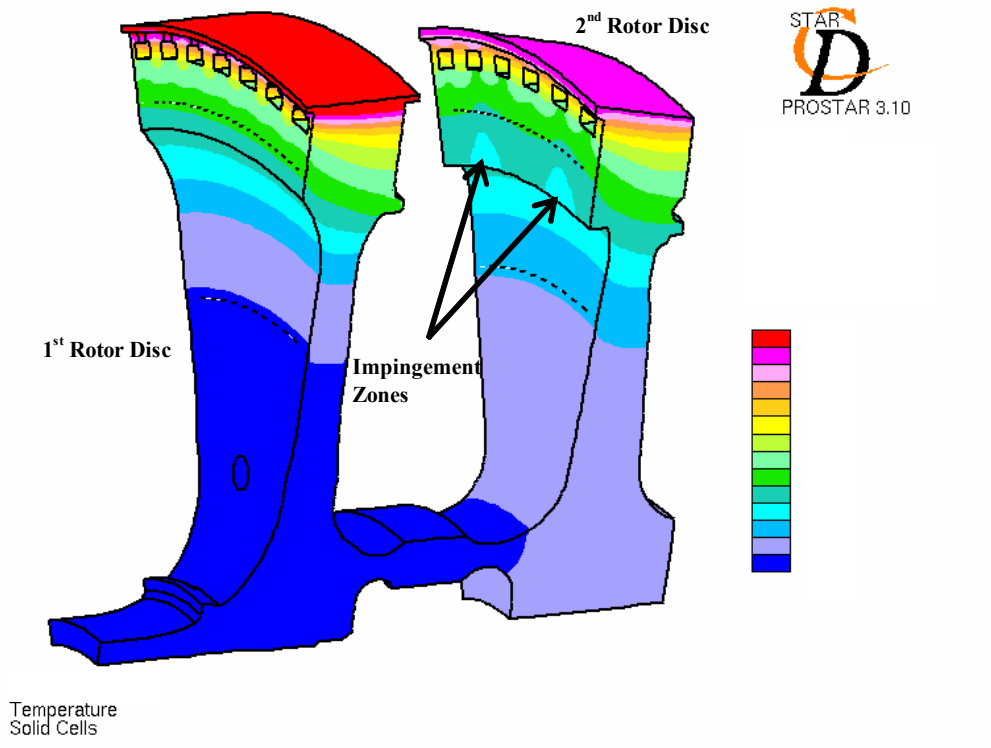

Figure 14: Metal temperature (Simplified N-S analysis)

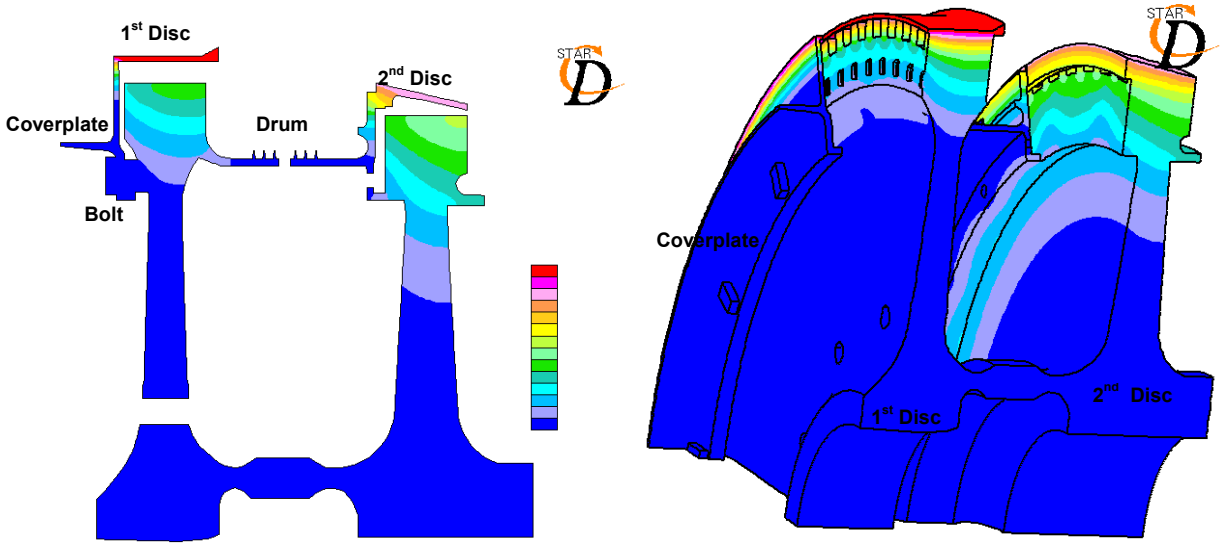

Figure 15: Metal Temperature (Detailed N-S analysis)

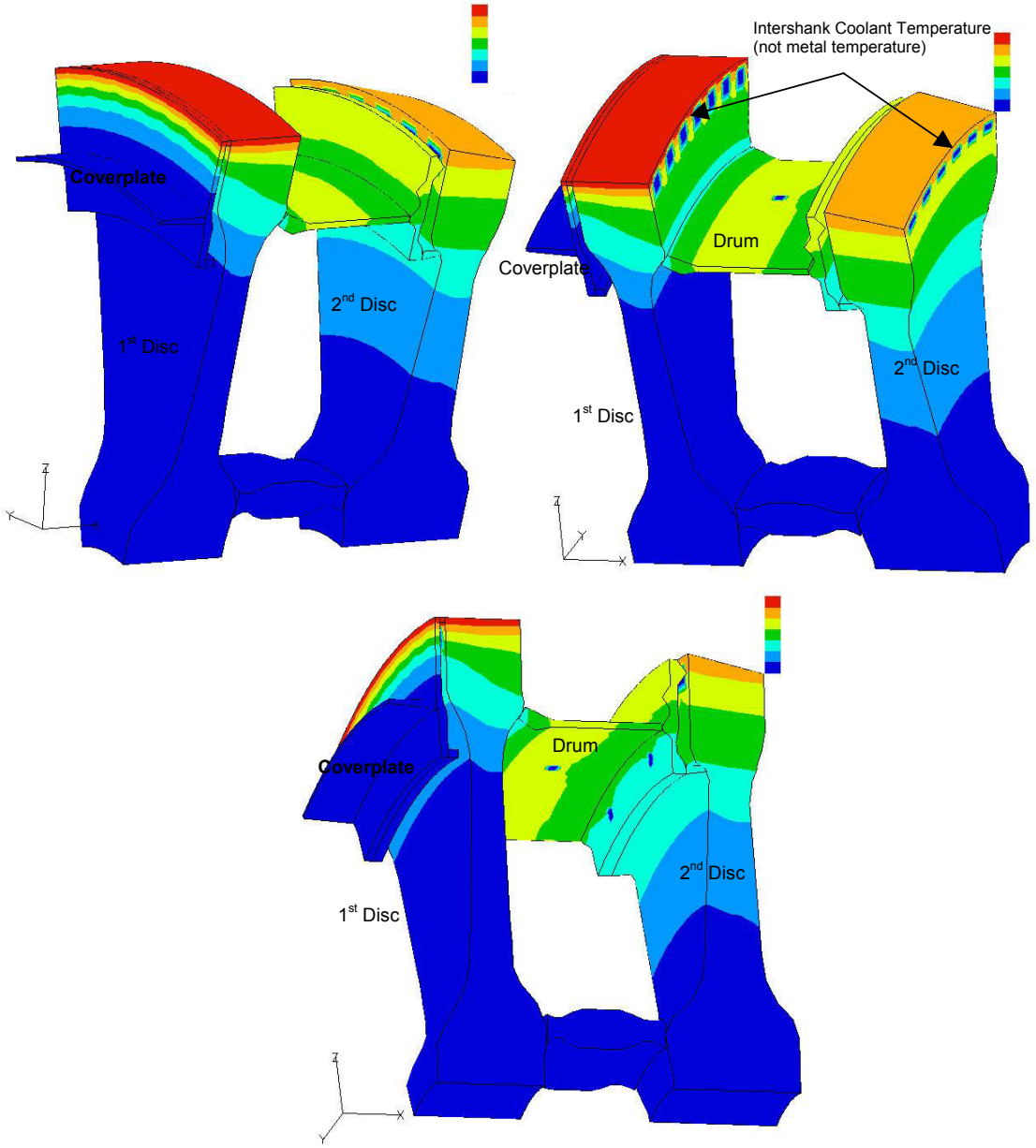

Figure 16: Disc Assembly Metal Temperature Distribution from Simplified Coupled Analysis (colour bands 75 K starting from the same point as those of the preceding figures)

Comparison of Temperature Results

A comparison of the temperature distributions for the three models is interesting (see figures 14, 15 and 16). The temperature contours for the coupled analysis are equivalent in value to every second contour in the N-S analyses. Care must be taken while comparing figure 14 to the upper left in figure 16 to realise that no coverplate is plotted on either disc in figure 14, while figure 16 has both, obscuring the disc face temperature contours beneath. There is very good agreement both in trend and level between the results of the two simplified analyses for the 1st disc, with the simplified coupled analysis consistently about 20 K below the N-S result. Figure 17 shows a temperature distribution comparison up the front face of the 1st disc for the two techniques as well as OEM thermal paint data. The sudden steep gradient at radii above about 0.225 m represents the blade shanks. The two analysis techniques overpredict the temperature distribution relative to the thermal paint because the temperature at which the rim of the "disc" (in reality the blade platform at the top of the shank) is fixed in the two analyses is in fact the predicted hot gas temperature at the hub. Future analyses will include the convective heat transfer at the platform instead of assuming the platform to be the gas temperature.

The simplified N-S analysis of Snedden (2003) and both subsequent analyses differ in that the bounding temperature on the 1st disc was reduced by some 40 K explaining why the simplified N-S predicts higher disc temperatures than the coupled technique at higher radii.

Also the discrepancy at lower radii, implying a difference in coolant temperature, is explained by the coupled technique using a total temperature for coolant supply, whereas the simplified N-S solution made use of the same value but as a static temperature in the coolant supply jets, implying a higher total temperature.

The results of the detailed N-S solution (Figure 16 and 18) are significantly colder than either of the other solutions or the thermal paint as a result of the approximately 60˚ reduction in coolant temperature entering from the modified boundary condition. The general trend is however the same.

The 2nd disc temperature penetrates to a slightly lower radius in the coupled analysis than in the N-S analysis. It is believed to be then result of

- neglecting impingement cooling on the front face of the second disc in the coupled analysis, and
- modelling the 2nd disc coverplate in the simplified N-S analysis as adiabatic and so not being heated by labyrinth seal leakage flow, leading to lower coolant temperatures than would otherwise be the case.

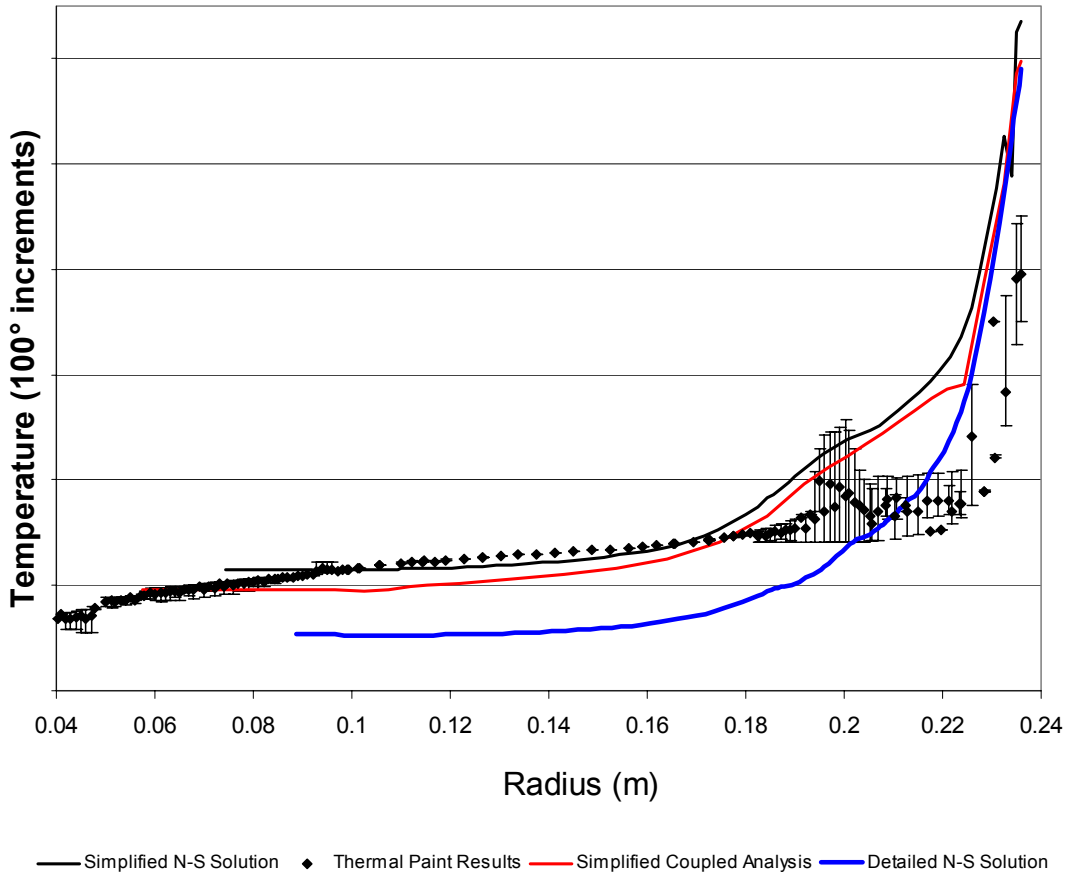

Figure 17: Graph of metal temperature on the front face of the 1st disc

Conclusions

As is clear from the results presented above it is possible to achieve accurate results with all the methods presented. The accuracy is largely a measure of the boundary conditions (such as can be seen in the detailed N-S solution, where the modeling of the coolant supply into the entrance cavity has a strong effect on the temperature of the coolant seen by the 1st disc and hence results in a 50˚ under prediction of the disc temperature as one proceeds toward the hub) or the modeling assumptions or simplifications (such as the failure of the simplified coupled model to capture the impingement zones on the 2nd disc). Despite these inherent inaccuracies in the models the agreement to the limited validation data available is good and the agreement or lack of agreement between methods easily attributed to the boundary conditions.

The results of this comparative study have in general terms confirmed the CSIR's approach toward this problem as outlined earlier: the technique of a simplified coupled solver used to provide quick and accurate solutions with transient capability and the N-S method used only to study relatively small sections of a disc cavity to determine the need or approach to resolving the flow in that area in the simplified coupled analysis.

To illustrate this conclusion it has been shown from the above analyses that the simplified coupled solver approach is arguably the most accurate approach when looking at the 1st disc alone, where the physics are well understood and modeled. In addition the simplified coupled solver method is quick to set-up and solve and capable of producing transient solutions crucial for mission analysis and component life predictions in similarly short timescales, not plausible for N-S solutions.

Only Figure12, as complicated as it is, shows the real worth of the N-S solutions, on close examination the 3D aspects resulting from the bolts, locking plate tabs and impingement zones can be seen. But this comes at enormous computational expense and despite an order of magnitude increase in grid size it still does not capture the geometry without simplification and satisfactory resolution expressed in terms of y+. Additionally much of the complexity leads to almost no substantial effect on the temperature or temperature gradients (important to life predictions) in the metal as conduction through the metal surface quickly eradicates the slight differences in say the heat transfer downstream of a bolt head. Should one wish to pursue a N-S solution to this problem in the future one would achieve an acceptable metal temperature distribution with a simplified geometry as used by Snedden (2003) with improved modeling of the inlet boundary condition and more emphasis on achieve grid independence and acceptable y+.

Acknowledgements

The authors would like to thank the Defence Research and Development Board of the South African Department of Defence for the funding to participate in this research

References

Gaugler RE (1978) *TACT1, A Computer Program for the Transient Thermal Analysis of a Cooled Turbine Blade or Vane Equipped with a Coolant Insert*, NASA TP 1271

Lippert A (1995) *Numerical Prediction of Internal Coolant Flow in Gas Turbine Blades*, M Eng Thesis, University of Pretoria, South Africa

Meitner PL (1989) *Computer Code for Predicting Coolant Flow and Heat Transfer in Turbomachinery*, AVSCOM TR No 89-C-008

Northrop A and Owen JM (1988), *Heat Transfer Measurements in Rotating-Disc Systems; Part 2: The Rotating Cavity with a Radial Outflow of Cooling Air*, International Journal of Heat and Fluid Flow, Vol 9, No 1

Owen JM, Haynes CM and Bailey FJ (1974), *Heat Transfer from an Air-Cooled Rotating Disc*", Proceedings of the Royal Society of London, Volume 336, p453-473

Owen JM and Haynes CM (1976), *Design Formulae for the Heat Loss and Frictional Resistance of Air-Cooled Rotating Discs*", Improvements in Fluid Machines and Systems for Energy Conversion, Volume 4, Hoepli, Milan, p127

Snedden GC (2003) *Quasi-3D Flow Simulation of a Real Disc Cavity with Conjugate Heat Transfer* ISABE-2003-1179

Snedden GC and Lambert T (2003) *A CFD Analysis Of the Impingement Cooling Effect of the Coolant Jet Caused by the T56 1st Stage Disc Metering Hole* ISABE-2003-1065